AMERICAN SOCIETY FOR MICROBIOLOGY | mBio®

RESEARCH ARTICLE

Aspergillus fumigatus Trehalose-Regulatory Subunit Homolog Moonlights To Mediate Cell Wall Homeostasis through Modulation of Chitin Synthase Activity

Arsa Thammahong, Alayna K. Caffrey-Card, Sourabh Dhingra, Joshua J. Obar, Robert A. Cramer

Department of Microbiology and Immunology, Geisel School of Medicine at Dartmouth, Hanover, New Hampshire, USA

ABSTRACT Trehalose biosynthesis is found in fungi but not humans. Proteins involved in trehalose biosynthesis are essential for fungal pathogen virulence in humans and plants through multiple mechanisms. Loss of canonical trehalose biosynthesis genes in the human pathogen *Aspergillus fumigatus* significantly alters cell wall structure and integrity, though the mechanistic link between these virulence-associated pathways remains enigmatic. Here we characterize genes, called *tslA* and *tslB*, which encode proteins that contain domains similar to those corresponding to trehalose-6-phosphate phosphatase but lack critical catalytic residues for phosphatase activity. Loss of *tslA* reduces trehalose content in both conidia and mycelia, impairs cell wall integrity, and significantly alters cell wall structure. To gain mechanistic insights into the role that TslA plays in cell wall homeostasis, immunoprecipitation assays coupled with liquid chromatography-tandem mass spectrometry (LC-MS/MS) were used to reveal a direct interaction between TslA and CsmA, a type V chitin synthase enzyme. TslA regulates not only chitin synthase activity but also CsmA sub-cellular localization. Loss of TslA impacts the immunopathogenesis of murine invasive pulmonary aspergillosis through altering cytokine production and immune cell recruitment. In conclusion, our data provide a novel model whereby proteins in the trehalose pathway play a direct role in fungal cell wall homeostasis and consequently impact fungus-host interactions.

IMPORTANCE Human fungal infections are increasing globally due to HIV infections and increased use of immunosuppressive therapies for many diseases. Therefore, new antifungal drugs with reduced side effects and increased efficacy are needed to improve treatment outcomes. Trehalose biosynthesis exists in pathogenic fungi and is absent in humans. Components of the trehalose biosynthesis pathway are important for the virulence of human-pathogenic fungi, including *Aspergillus fumigatus*. Consequently, it has been proposed that components of this pathway are potential targets for antifungal drug development. However, how trehalose biosynthesis influences the fungus-host interaction remains enigmatic. One phenotype associated with fungal trehalose biosynthesis mutants that remains enigmatic is cell wall perturbation. Here we discovered a novel moonlighting role for a regulatory-like subunit of the trehalose biosynthesis pathway in *A. fumigatus* that regulates cell wall homeostasis through modulation of chitin synthase localization and activity. As the cell wall is a current and promising therapeutic target for fungal infections, understanding the role of trehalose biosynthesis in cell wall homeostasis and virulence is expected to help define new therapeutic opportunities.

KEYWORDS *Aspergillus fumigatus*, cell wall, chitin, filamentous fungi, pathogenesis, trehalose

Received 11 January 2017 **Accepted** 7 April 2017 **Published** 25 April 2017

Citation Thammahong A, Caffrey-Card AK, Dhingra S, Obar JJ, Cramer RA. 2017. *Aspergillus fumigatus* trehalose-regulatory subunit homolog moonlights to mediate cell wall homeostasis through modulation of chitin synthase activity. mBio 8:e00056-17. https://doi.org/10.1128/mBio.00056-17.

Editor Tamara L. Doering, Washington University School of Medicine

Address correspondence to Robert A. Cramer, Robert.A.Cramer.JR@dartmouth.edu.

Aspergillus fumigatus is a filamentous fungus that can cause a severe fungal disease, invasive aspergillosis (IA), in immunocompromised humans (1, 2). Azoles are antifungal drugs that inhibit fungal ergosterol synthesis and are the current drugs of choice for IA treatment. Drug-drug interactions, undesirable side effects, and a growing emergence of azole-resistant strains in certain parts of the world are challenges faced by clinicians employing azole therapy against IA (3, 4). Thus, there is a growing need for new antifungal drugs to combat life-threatening infections caused by *A. fumigatus* and associated species.

Trehalose biosynthesis is found in many organisms, e.g., insects, plants, invertebrates, and fungi, but not in humans. The canonical fungal trehalose biosynthesis pathway was defined in *Saccharomyces cerevisiae* (5, 6). The canonical pathway in *S. cerevisiae* consists of the following components: Tps1p (trehalose-6-phosphate synthase), Tps2p (trehalose-6-phosphate phosphatase), and two regulatory subunits, Tps3p and Tsl1p (5–11). These proteins form a complex to produce trehalose (5, 6). Genes encoding trehalose biosynthesis proteins are essential for virulence in the human-pathogenic yeasts *Candida albicans* (12) and *Cryptococcus neoformans* (13). Canonical fungal trehalose biosynthesis is also present in *A. fumigatus*. In *A. fumigatus*, *tps1* has at least two paralogs that are important for trehalose production, *tpsA* and *tpsB* (*tpsA/B*) (14), whereas Tps2 has one ortholog, named OrlA (15). While loss of *tpsA* and *tpsB* enhances the virulence of *A. fumigatus* as measured by murine mortality and immunopathogenesis, the loss of *orlA* significantly attenuates virulence (14, 15). A striking feature of both the *tpsA/B* and *orlA* genetic mutants and of yeast trehalose mutants is their altered cell wall integrity. However, the mechanism(s) through which trehalose biosynthesis proteins impact fungal cell wall homeostasis is undefined. Given the extensive interactions between trehalose biosynthesis and basic fungal carbon metabolism, both indirect and direct mechanisms are plausible, though not mutually exclusive, causative models.

In this study, characterization of the unstudied *A. fumigatus* trehalose regulatory subunits *tslA* and *tslB* revealed a surprising role for TslA in modulating fungal cell wall homeostasis. Our results support a model whereby TslA plays a critical direct role in fungal cell wall homeostasis through modulating the localization and activity of a class V chitin synthase enzyme, CsmA. Thus, for the first time, our results provide novel insights into mechanisms through which the canonical fungal trehalose biosynthesis pathway directly impacts fungal cell wall homeostasis and consequently the host-pathogen interaction.

RESULTS

TslA and TslB are homologs of yeast trehalose regulatory subunits Tsl1 and Tps3. To identify putative regulatory subunits of the trehalose complex in *A. fumigatus*, we queried the protein sequences of *S. cerevisiae* Tsl1p and Tps3p against the *A. fumigatus* strain A1163 protein database using BLASTp algorithms (http://www.aspergillusgenome.org/). Two proteins, AFUB_089470 and AFUB_021090, showed significant sequence similarity to Tsl1p and Tps3p and were consequently named TslA and TslB, respectively. TslA contains 919 amino acids, while TslB contains 918 amino acids. The TslA and Tsl1p and Tps3p protein sequences showed 40% and 37% amino acid identity and 59% and 54% protein sequence similarity, respectively. TslB and Tsl1p and Tps3p showed 38% and 36% amino acid identity and 57% and 53% protein sequence similarity, respectively. Protein domain analyses revealed that TslA and TslB share domains similar to those of the trehalose-6-phosphate phosphatase (TPP) OrlA, such as the glycosyl transferase domain (GT1-TPS) and the halogen-associated dehydrogenase-like domain (HAD-TPP), as previously reported in *A. niger* (16). However, compared to the known catalytic sites of TPS and TPP domains in bacteria (17, 18), TslA and TslB appear to lack catalytic residues of both domains similar to those of yeast Tsl1p and Tps3p. To study the function of these proteins in *A. fumigatus*, we generated genetic single- and double-null mutants of *tslA* and *tslB* in *A. fumigatus* CEA17 (mutants Δ*tslA*, Δ*tslB*, and Δ*tslA/B*) as previously described (19–21). Reconstituted Δ*tslA* and Δ*tslB*

strains were generated by ectopic insertion of the wild-type *tslA* and *tslB* alleles (Δ*tslA*+*tslA* and Δ*tslB*+*tslB*) (22). Singly reconstituted Δ*tslA*/*B* strains were also generated using either wild-type *tslA* alleles or wild-type *tslB* alleles (Δ*tslA*/*B*+*tslA* or Δ*tslA*/*B*+*tslB*) (22). All strains were confirmed by both PCR and Southern blot analyses. Furthermore, the confirmed strains were analyzed with quantitative reverse transcriptase PCR (qRT-PCR) and mRNA corresponding to *tslA* and *tslB* was confirmed to be absent in all mutants and confirmed to be restored to wild-type levels in the respective reconstituted strains (data not shown). In Δ*tslA*, we observed increased mRNA levels *of tslB*; *tslA* mRNA levels remained similar to the wild-type levels in the Δ*tslB* mutant (data not shown).

Loss of TslA and TslB decreases trehalose content and delays germination. To test the hypothesis that TslA and TslB are involved in trehalose biosynthesis in *A. fumigatus*, we measured conidia and mycelium trehalose content in our wild-type and generated strains (Fig. 1). A significant decrease in trehalose content in the Δ*tslA*, Δ*tslA*/*B*, and Δ*tslA*/*B*+*tslB* strains was observed compared to levels observed with the wild-type and reconstituted strains in both the conidial and mycelial stages (Fig. 1). Loss of TslB alone had minimal impact on trehalose levels in conidia or mycelia. These results suggest that TslA is more critical for trehalose production than TslB. However, loss of TslB in Δ*tslA* further reduced trehalose content compared to that seen with Δ*tslA* alone ($P < 0.0001$). This result suggests that TslB is also involved in trehalose production (Fig. 1).

Loss of trehalose biosynthesis in *A. fumigatus* and other filamentous fungi affects germination of conidia (14, 15, 23). Consistent with previous observations, the Δ*tslA*, Δ*tslB*, and Δ*tslA*/*B* strains showed a significant delay in germination in the first 8 h when cultured in liquid glucose minimal medium (LGMM). At 8 h, the wild-type strain germinated at 94.00 ± 2.00% whereas the Δ*tslA*, Δ*tslB*, and Δ*tslA*/*B* strains germinated at 80.33 ± 2.08% ($P = 0.0012$), 86.00 ± 3.46% ($P = 0.0257$), and 86.67 ± 2.31% ($P = 0.0142$), respectively. Nevertheless, these mutants showed no detectable differences in radial growth on solid GMM or in biomass in batch culture at 37°C compared to the levels seen with the wild-type and reconstituted strains.

Loss of TslA increases susceptibility to cell wall-perturbing agents. Trehalose biosynthesis null mutants have associated cell wall defects in *A. fumigatus* as evidenced by data from Δ*tpsA*/*B* and Δ*orlA* strains (14, 15). To test the hypothesis that TslA and TslB play a role in cell wall homeostasis, we utilized the cell wall-perturbing agents Congo red (CR), calcofluor white (CFW), and caspofungin (CPG). We observed increased CR and CFW susceptibility with the Δ*tslA* and Δ*tslA*/*B* strains (Fig. 2A). No significant difference in CPG susceptibility was observed. To further confirm the cell wall phenotypes of these mutants, we utilized osmostabilizing medium containing 1.2 M sorbitol (sorbitol minimal media [SMM]) and an enriched medium, Sabouraud dextrose agar (SDA). Δ*tslA* showed restored cell wall phenotypes on both SMM and SDA in the presence of CFW (Fig. 2B). As both CR and CFW bind to chitin on the cell wall and inhibit growth, while CPG inhibits β-1,3-glucan synthase, these results suggest that loss of TslA affects the chitin component of the fungal cell wall.

Loss of TslA alters cell wall structure and exposure of fungal cell wall microbe-associated molecular patterns (MAMPs). One possible mechanism to explain the increased susceptibility of the Δ*tslA* strain to cell wall-perturbing agents is an inherent alteration in cell wall structure. To explore this hypothesis, transmission electron microscopy (TEM) was utilized. TEM micrographs revealed that the Δ*tslA* strain had a significantly thinner cell wall than the wild type ($P = 0.002$) (Fig. 3). Moreover, an accumulation of an electron-dense material near the cell wall of the Δ*tslA* strain was observed along the hyphae. We hypothesize that loss of TslA may alter extracellular matrix and/or associated cell wall proteins of this fungus. Given the significant alteration in the Δ*tslA* strain cell wall structure, we next tested the hypothesis that exposure of key MAMPs, chitin and β-glucan, is altered in this mutant.

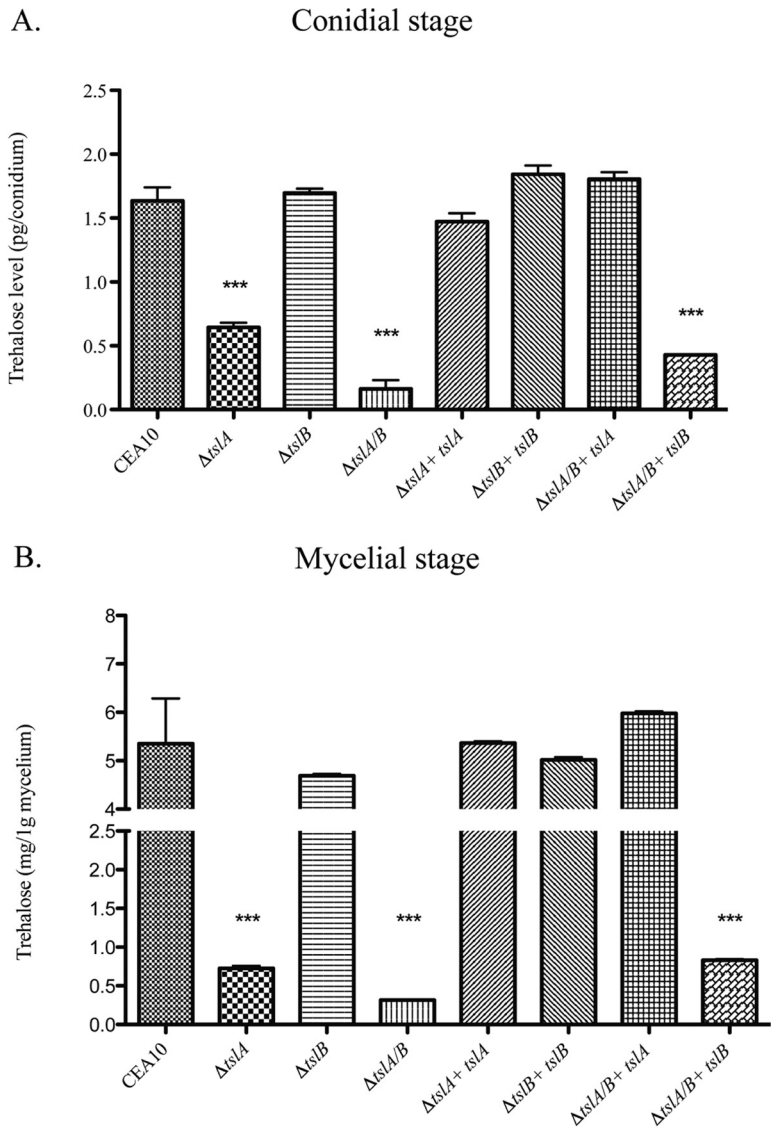

FIG 1 Loss of TslA and TslB decreases trehalose production in both conidia (A) and hyphae (B). Quantitation of trehalose production in conidia and mycelia was performed using glucose oxidase (GO) assays (Sigma) after trehalase enzyme incubation. For the conidial stage, 2×10^8 conidia were used to extract trehalose by boiling at 100°C for 20 min and collecting the supernatant to perform GO assays. For the mycelial stage, 1×10^8 conidia were cultured in 10 ml LGMM at 37°C for 16 h, the mycelia were weighed and lyophilized, and trehalose extraction was performed. Data are presented as means ± SE of results from three biological replicates. ***, $P < 0.0001$ (unpaired two-tailed Student's *t* test compared to the wild-type CEA10 results).

CFW and wheat germ agglutinin (WGA) staining were used to observe chitin levels and exposure on the cell wall. Loss of TslA dramatically increased both CFW staining and WGA staining, which likely reflects increased chitin content of this mutant ($P = 0.0074$ for CFW and $P = 0.0017$ for WGA) (Fig. 4A and B). Soluble dectin-1 (s-dectin-1) staining was used to observe β-glucan exposure, and loss of TslA significantly decreased s-dectin-1 staining on fungal germlings ($P = 0.0005$) (Fig. 4C). We conclude that loss of TslA affects cell wall homeostasis in part by disrupting chitin and β-glucan homeostasis.

One possible explanation of these results is that loss of TslA indirectly affects the fungal cell wall through induction of a cell wall integrity response that is perhaps due to an alteration in intracellular osmotic homeostasis resulting from reductions in trehalose levels. To test this hypothesis, we utilized qRT-PCR to quantitate mRNA levels

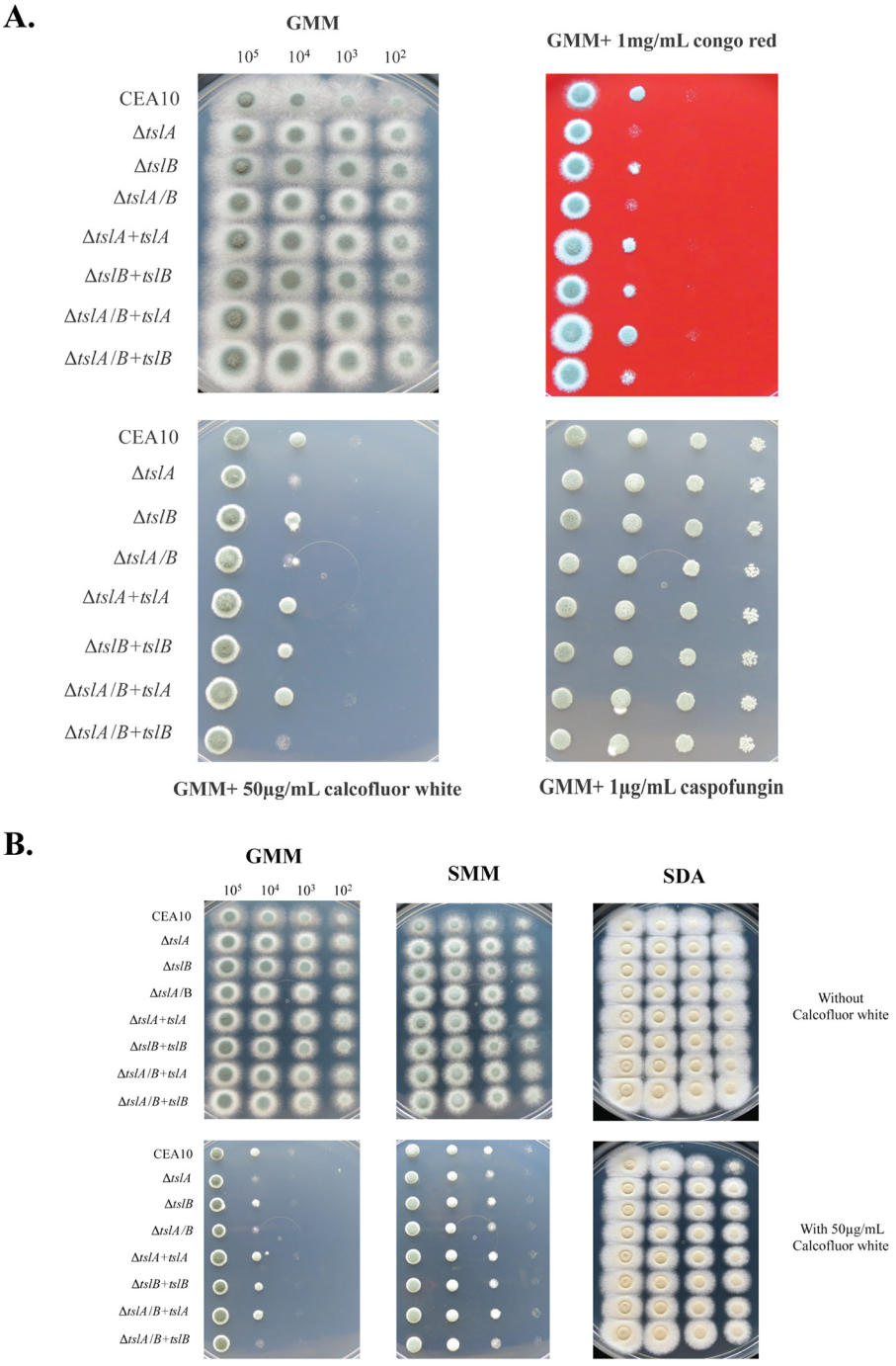

FIG 2 Loss of TslA increases fungal susceptibility to cell wall-perturbing agents (A), and growth of the Δ*tslA* strain is restored on sorbitol minimal media (SMM) and Sabouraud dextrose media (SDA) in the presence of 50 μg/ml calcofluor white (B). Dropout assays were performed at 37°C for 2 days by using 10^5 to 10^2 conidia for each strain inoculated on GMM with or without cell wall-perturbing agents, i.e., 1 mg/ml Congo red, 50 μg/ml calcofluor white, and 1 μg/ml caspofungin. Images and data are representative of three independent experiments with similar results.

of transcription factors known to be induced by cell wall stress, *rlmA* and *atfA* (24, 25). We observed that the mRNA levels of both *rlmA* and *atfA* in the Δ*tslA* strain were equivalent to the levels seen with the wild type and the reconstituted strains with or without the presence of CFW (Fig. 5A). Alternatively, it is possible that loss of TslA alters carbon metabolic flux and thus affects cell wall biosynthesis. Several studies in multiple fungi have observed significant changes in cell wall biosynthesis-encoding gene mRNA

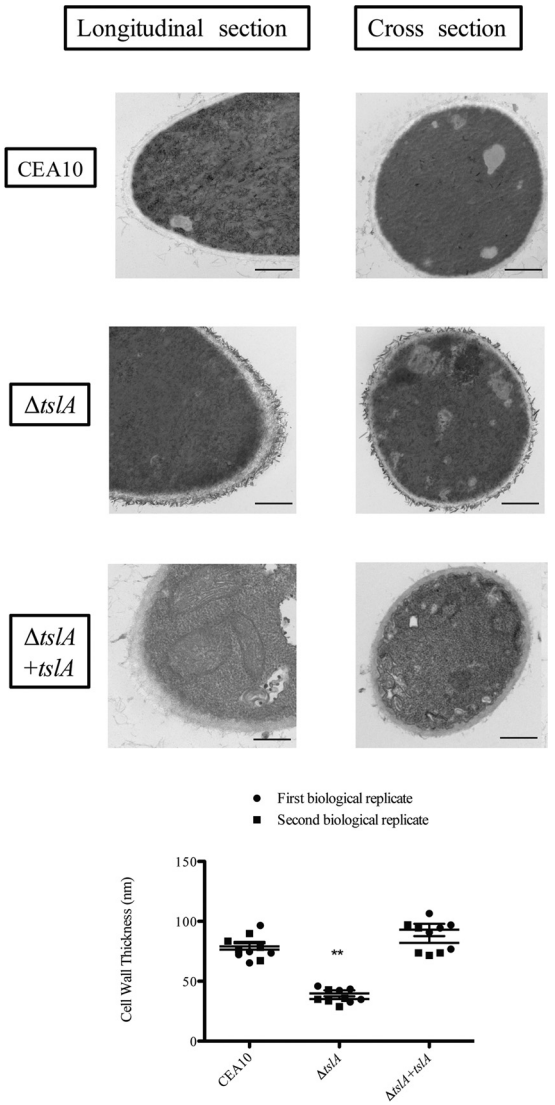

FIG 3 Loss of TslA decreases fungal cell wall thickness and results in accumulation of electron-dense material at the outer layer of the cell wall. Mycelia from each strain were prepared for TEM as previously described (19, 39). Cell wall thickness was analyzed by ImageJ. Data are presented as means ± SE of 10 measurements from two biological replicates of each strain. **, P value = 0.002 (unpaired two-tailed Student's t test compared to the wild-type CEA10 results). Bars, 500 nm.

levels in response to nutrient availability (26–29). To investigate this hypothesis, we analyzed the mRNA levels of *fksA*, encoding a β-glucan synthase enzyme, and of *csmA*, encoding a class V chitin synthase enzyme, using qRT-PCR. We observed no change in the expression levels of these genes in the Δ*tslA* strain (Fig. 5B). The combination of osmostabilizing medium rescue of the cell wall perturbation phenotype, lack of an intrinsic cell wall integrity response, and lack of changes in cell wall biosynthesis-encoding gene mRNA levels suggests that changes in the cell wall homeostasis resulting from the loss of TslA are unlikely to be solely the result of altered carbon metabolism.

TslA interacts with a class V chitin synthase enzyme. To understand the mechanism behind the role of TslA in cell wall homeostasis, we utilized an affinity purification approach to identify proteins interacting with TslA. To utilize this approach, we generated a TslA C-terminal S-tag strain (30, 31). Similar to previous observations in *S. cerevisiae*, we observed that TslA interacts with the TPP, OrlA, which suggests that TslA may regulate TPP activity/function in *A. fumigatus* (see Table S2 in the supple-

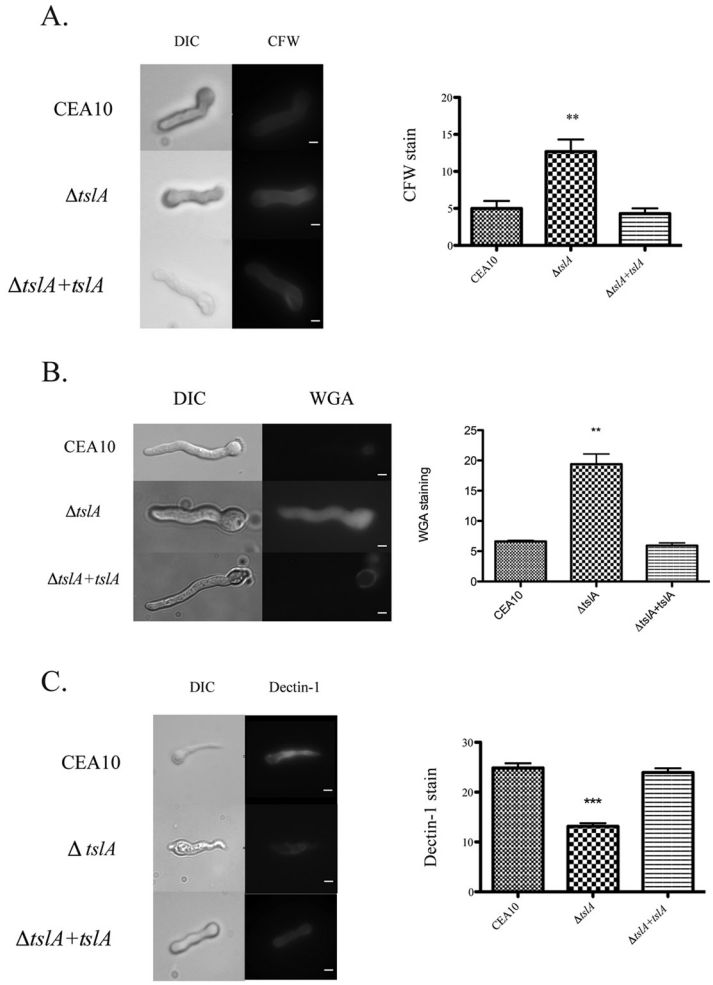

FIG 4 Loss of TslA alters MAMP cell wall exposure. (A and B) The Δ*tslA* strain has increased chitin levels/exposure as measured by calcofluor white (CFW) staining (A) or wheat germ agglutinin (WGA) (B) compared to the results seen with wild-type CEA10 and the reconstituted Δ*tslA*+*tslA* strain. Each strain was cultured into the germling stage under normoxic conditions at 37°C. The germlings were UV irradiated and stained with 25 μg/ml CFW or with 5 μg/ml WGA. The mean intensity was analyzed using ImageJ and the corrected total cell fluorescence (CTCF) was calculated (69, 70). **, *P* value = 0.0074 for CFW and 0.0017 for WGA compared to CEA10 (unpaired two-tailed Student's *t* test compared to the wild-type CEA10 results). DIC, differential interference contrast. (B) The Δ*tslA* strain has decreased β-glucan exposure as measured by s-dectin-1 staining compared to the wild-type CEA10 and the reconstituted Δ*tslA*+*tslA* strain. Each strain was cultured to the germling stage under normoxic conditions at 37°C. The germlings were UV irradiated, blocked, and stained with a conditioned medium containing s-dectin1-hFc followed by Alexa Fluor 488-conjugated, goat anti-human IgG1. The corrected total cell fluorescence (CTCF) was calculated. ***, *P* value = 0.0005 (unpaired two-tailed Student's *t* test compared to the wild-type CEA10 results). Data are presented as means ± SE of 15 images from three biological replicates. Bar, 3 μm.

mental material). TslA also interacted with metabolic enzymes involved in central carbon metabolism, including proteins in glycolysis and pentose phosphate pathways. Unexpectedly, TslA interacted with the chitin synthase enzyme, CsmA (ChsE; AFUB_029080). These data suggest that TslA has important metabolism regulatory functions in addition to the canonical function in trehalose biosynthesis. A list of TslA interacting proteins, with score and identity notations, is presented in Table S2.

To validate the protein-protein interaction between TslA and CsmA, we utilized a coimmunoprecipitation (Co-IP) approach (Fig. 6). We first introduced a 3× Flag tag to the C terminus of CsmA in the background of the wild-type and S-tagged TslA strains. We observed no changes in the phenotypes and trehalose levels of these tagged strains compared to wild-type levels (data not shown). We performed coimmunoprecipitation

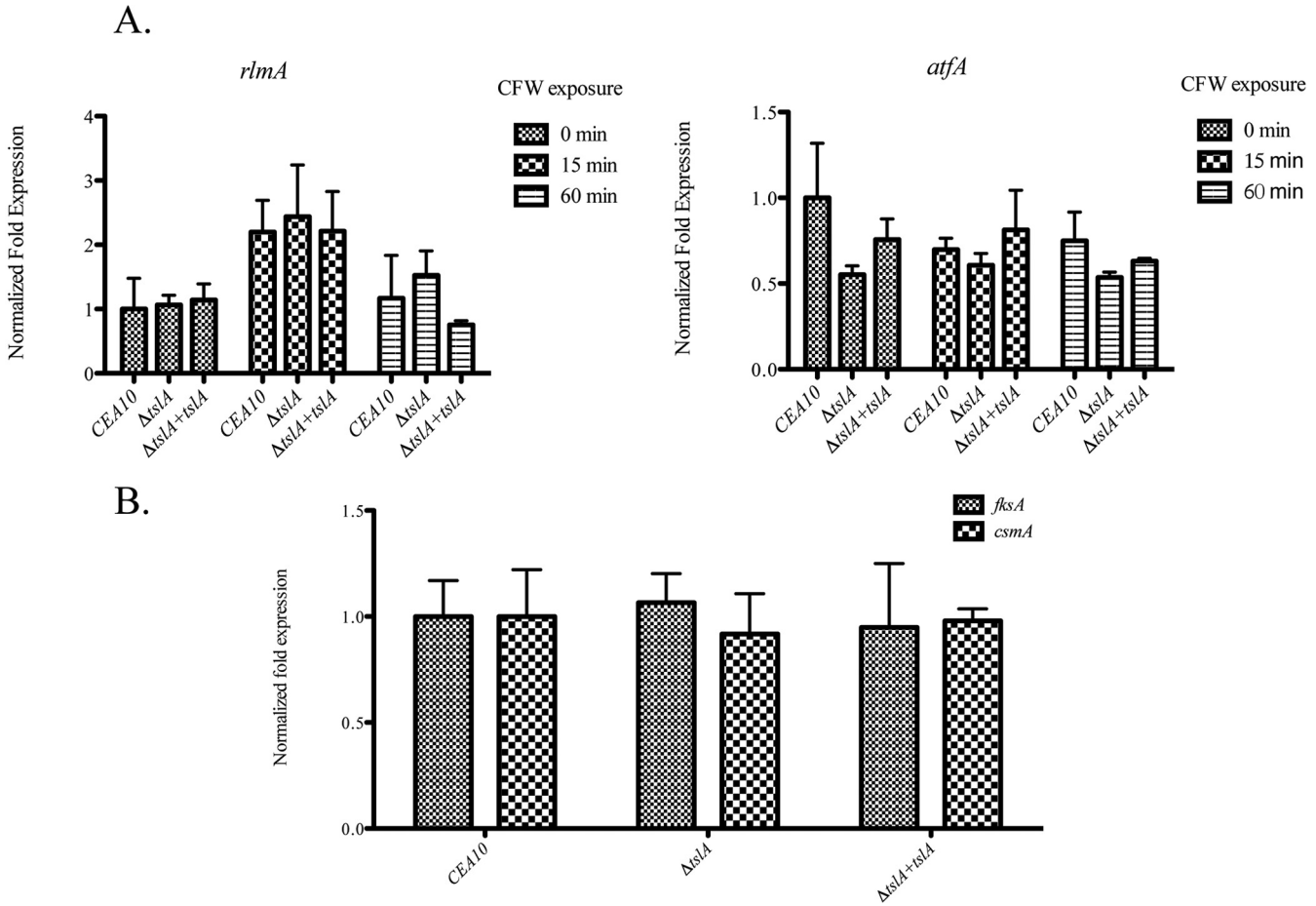

FIG 5 Loss of TslA does not affect the cell wall integrity and HOG-MAPK pathways (A) and does not change the expression of *fksA* and *csmA* (B). A total of 10^6 conidia of the wild-type strain and the Δ*tslA* strain were incubated overnight in liquid GMM, and CFW was added for 0, 15, and 60 min as indicated. Samples were collected, and RNA extraction was performed for measuring *rlmA*, *atfA*, *fksA*, and *csmA* mRNA abundance using qRT-PCR analysis as previously described (15). Data are presented as means ± SD of results from three biological replicates of each strain.

assays using S-protein beads with the wild-type, S-tagged TslA, and Flag-tagged CsmA strains and the S-tagged TslA and Flag-tagged CsmA strain. Using Western blot analysis, we observed that TslA coimmunoprecipitated from only the S-tagged TslA strain and the S-tagged TslA and Flag-tagged CsmA strain. In support of the affinity purification data, CsmA coimmunoprecipitated in the S-tagged TslA and Flag-tagged CsmA strain (Fig. 6A). To further confirm the interaction between TslA and CsmA, we performed reciprocal coimmunoprecipitation assays using anti-Flag M2 magnetic beads. We observed CsmA to coimmunoprecipitate from only the Flag-tagged CsmA strain and the S-tagged TslA and Flag-tagged CsmA strains. Also, TslA was coimmunoprecipitated from the S-tagged TslA and Flag-tagged CsmA strains (Fig. 6B). From these results, we conclude that TslA and CsmA physically interact in *A. fumigatus*.

Loss of TslA increases chitin synthase activity and affects cellular localization of CsmA. One potential mechanism to explain our results is that TslA directly regulates chitin synthase activity through CsmA. To test the hypothesis that TslA regulates CsmA activity, we utilized a nonradioactive chitin synthase activity approach successfully utilized in *A. fumigatus* (32, 33). After extracting membrane proteins and incubating with substrates for chitin production, we observed a significant increase in chitin production in the Δ*tslA* strain compared to the wild-type, reconstituted, and control Δ*csmA* strains whereas the negative controls showed very low chitin content (Fig. 7) (for 10 μg, $P = 0.0117$ [for comparisons between the wild-type strain and the Δ*tslA* strain) and $P = 0.0013$ (for comparisons between the wild-type strain and the Δ*csmA* strain).

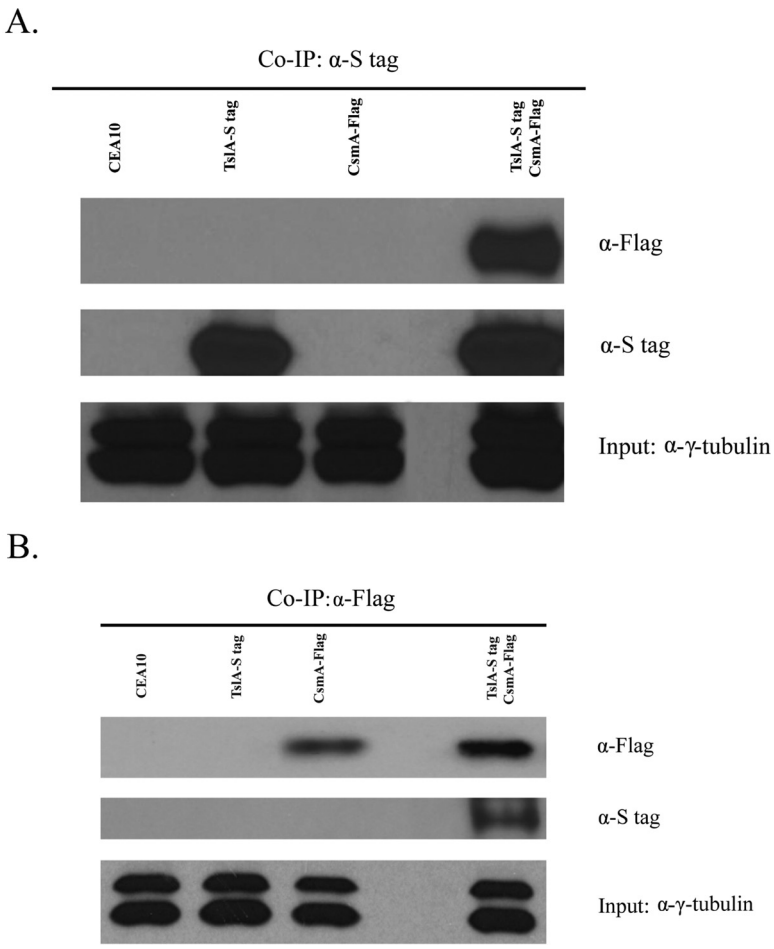

FIG 6 TslA physically interacts with CsmA. Affinity purification assays from Flag-tagged CsmA strains in the background of S-tagged TslA were performed with S-protein beads (A) and anti-Flag beads (B) to verify interactions. Data are images representative of results from three independent experiments, all with similar results.

This result supports the hypothesis that TslA is a potential negative regulator of chitin synthase activity through its interaction with CsmA.

As chitin synthase localization is critical for cell wall homeostasis in fungi, we hypothesized that TslA alters CsmA localization and, consequently, chitin synthase activity. To observe the change in the localization of CsmA, we introduced a green fluorescent protein (GFP) tag into the C terminus of CsmA in the wild-type and Δ*tslA* strain backgrounds. We confirmed the stability of the C-terminal GFP-tagged CsmA protein of each strain using Western blot analysis (Fig. 8A). Consistent with results in *A. nidulans*, CsmA primarily localized to the growing hyphal tips and septa in wild-type *A. fumigatus* (34). In contrast, the localizations of CsmA in the Δ*tslA* strain were dispersed along the lateral cell wall of the fungus and throughout the cytoplasm and were not spatially restricted to the hyphal tips or septa (Fig. 8B). Furthermore, to quantify the puncta at the subapex region (within 20 μm of the tip), the puncta in the images were analyzed, and fewer puncta were visible in the Δ*tslA* strain ($P < 0.0001$ [for comparisons between CEA10 and the Δ*tslA* strain]) (Fig. 8C). Consequently, we conclude that TslA is critical for proper CsmA localization at the hyphal tip and hypothesize that loss of TslA causes dysregulation of chitin synthase activity through altered CsmA localization. To gain further insight into how TslA affects CsmA localization, we investigated TslA localization using a strain with expression of C-terminal GFP-tagged TslA. We observed that TslA localized nonspecifically in the cytosol throughout the hyphae after 12 h or 16 h of incubation (Fig. 8D) (see Fig. S1 in the supplemental material).

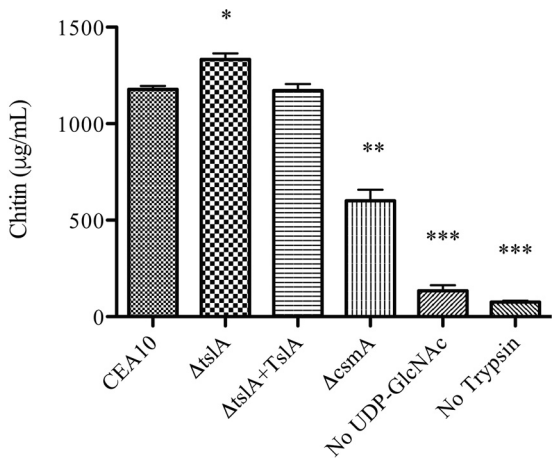

FIG 7 Loss of TslA increases chitin synthase activity. Ten micrograms of membrane proteins were used to perform a nonradioactive chitin synthase activity assay. Each strain was cultured at 30°C for 6 h and switched to 37°C for 24 h. Ten micrograms of the wild type's membrane proteins was used to compare with no substrate, UDP-N-acetyl glucosamine (UDP-GlcNAc) and no trypsin as negative-control assays. *, $P = 0.0117$; **, $P = 0.0013$; ***, $P < 0.0001$ (unpaired two-tailed Student's *t* test compared to the wild-type CEA10 results). Data are presented as means ± SE of results from three biological replicates.

TslA modulates the host inflammatory response. As the fungal cell wall is at the interface of the host-pathogen interaction, we next tested the hypothesis that loss of TslA impacts murine invasive pulmonary aspergillosis (IPA) outcomes. First, fungal virulence was assessed using a survival analysis in the chemotherapeutic murine model of IPA (35). From the survival experiment, all Δ*tslA* strain-inoculated mice perished by day 7, whereas the wild-type-strain-inoculated and reconstituted-strain-inoculated groups survived through the second week (Fig. 9A). The median durations of survival for mice inoculated with the wild type, the Δ*tslA* strain, and the reconstituted strain were 3, 3.5, and 3 days, respectively. Although the Δ*tslA* strain-inoculated mice had a clear trend toward earlier mortality than the mice in the groups inoculated with the wild-type strain or the reconstituted strain, Kaplan-Meier analysis showed no significant difference between groups ($P = 0.066$ [for comparisons between the wild-type and Δ*tslA* strain groups]). We next examined the pulmonary fungal burden of lung homogenates using a quantitative PCR (qPCR) approach to quantitate fungal 18S ribosomal DNA (rDNA) levels (36) and observed no significant difference between the results seen with the Δ*tslA* strain and the wild-type and reconstituted strains ($P = 0.057$ [for comparisons between the wild-type and Δ*tslA* groups) (Fig. 9B). However, significant differences in lung histopathology were observed between groups, with Δ*tslA*-inoculated mice containing increased levels of inflammatory foci compared to those inoculated with the wild-type and reconstituted strains (Fig. 9C). Moreover, the organizations of the inflammatory lesions were significantly different between the Δ*tslA* strain and the wild type, with many Δ*tslA* lesions exhibiting abscess-like characteristics, especially on day 4 after inoculation (Fig. 9C). We hypothesize that the trend toward higher mortality rates and earlier mortality of Δ*tslA*-inoculated mice was the result of increased immunopathogenesis and an altered host response.

We tested this hypothesis by collecting bronchoalveolar lavage fluid (BALF) on day 2 postinoculation (D2PI). Consistent with the histopathological findings, we observed larger inflammatory cell infiltrates from BALF of Δ*tslA*-inoculated mice than from BALF of the wild-type- or reconstituted-strain-inoculated groups ($P = 0.0051$ [for comparisons between CEA10 and the Δ*tslA* strain]) (Fig. 9D). Cell differential counts revealed increased infiltration of macrophages and neutrophils from the BALF of Δ*tslA*-inoculated mice compared to the results seen with the wild-type and reconstituted strains (for neutrophils, $P < 0.05$ [two-way analysis of variance {ANOVA} for comparisons among the CEA10, Δ*tslA*, and Δ*tslA*+*tslA* strains; for macrophages, $P < 0.01$

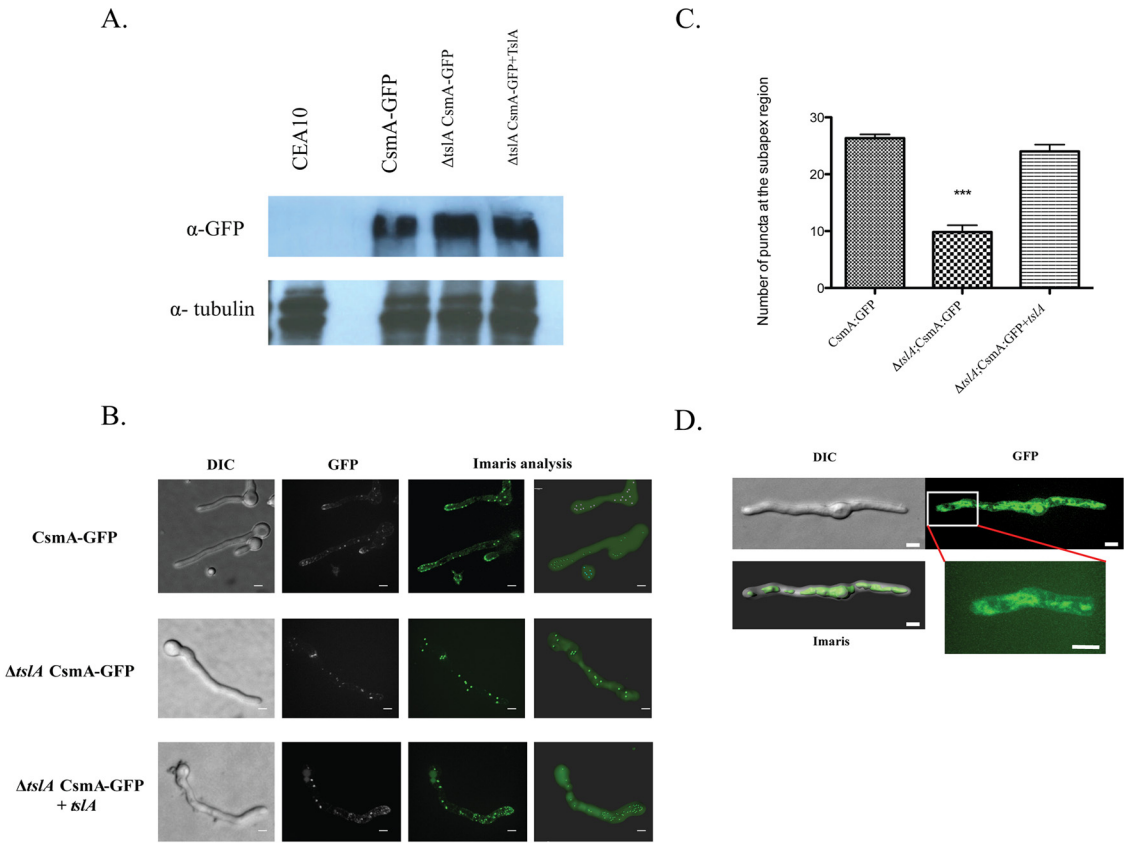

FIG 8 TslA promotes CsmA hyphal tip localization. (A) Western blot analysis of C-terminal GFP-tagged CsmA in the wild-type strain, Δ*tslA* strain, and Δ*tslA*+*tslA* strain backgrounds. (B) C-terminal GFP-tagged CsmA was generated in the wild-type strain, Δ*tslA*, and Δ*tslA*+*tslA* mutant backgrounds. Each strain was cultured at 37°C for 12 h, and live-cell imaging was performed using a Quorum Technologies WaveFX spinning disk confocal microscope (magnification, ×1,000). The images were analyzed using Imaris 8.1.4 software. (C) Loss of TslA changes the number of CsmA puncta at the hyphal tip. To quantify the puncta at the subapex region (within 20 μm of the tip), the puncta in the images were counted and analyzed using Imaris 8.1.4 software. ***, $P < 0.0001$ (unpaired two-tailed *t* test compared to the wild-type CEA10 results). (D) Localization of GFP-tagged TslA. C-terminal GFP-tagged TslA was generated and cultured at 37°C for 12 h. Live-cell imaging was performed using a Quorum Technologies WaveFX spinning disk confocal microscope (magnification, ×1,000). The three-dimensional (3D) structure of TslA puncta was created by the use of Imaris 8.1.4 software. Data are presented as means ± SE of results corresponding to 15 images from three biological replicates. Bar, 3 μm.

[two-way ANOVA for comparisons among the CEA10, Δ*tslA*, and Δ*tslA*+*tslA* strains]) (Fig. 9E).

To better understand potential causes of the higher levels of inflammatory cellular infiltrate inside Δ*tslA*-inoculated lungs, we utilized a Luminex assay to quantitate selected inflammatory cytokines from the BALF. Despite the equivalent levels of fungal burden, we observed an increased-inflammatory-cytokine profile, including increases in the levels of tumor necrosis factor alpha (TNF-α), CXCL1, and macrophage inflammatory protein 1-alpha (MIP-1α or CCL3), in Δ*tslA*-inoculated BALF compared to the wild-type and reconstituted-strain results. MIP-1α levels increased significantly in the Δ*tslA*-inoculated BALF ($P = 0.0286$) (Fig. 9F). Consequently, we conclude that the increased chitin levels and the decreased β-glucan levels on the cell wall of the Δ*tslA* strain alter the immunopathogenesis of murine IPA through increased and differential recruitment of inflammatory cells, likely through alterations in the secretion of proinflammatory cytokines.

DISCUSSION

The trehalose biosynthesis pathway is crucial for the virulence of human- and plant-pathogenic fungi, including *Candida albicans* (12), *Cryptococcus neoformans* (13), *Aspergillus fumigatus* (15), and *Magnaporthe oryzae* (37). In *A. fumigatus*, loss of the trehalose synthases TpsA and TpsB virtually eliminates trehalose production and results

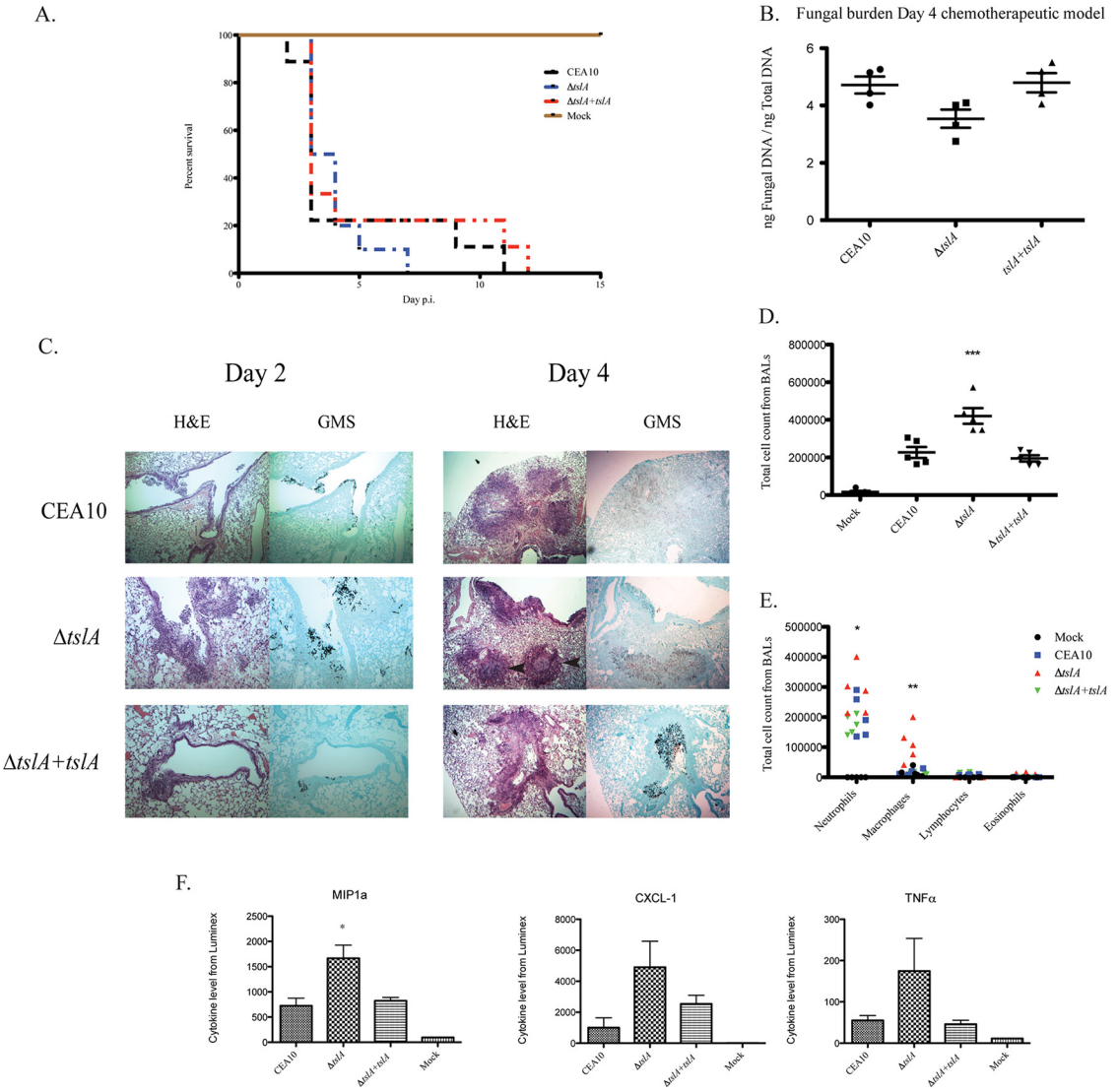

FIG 9 Survival analysis (A) and fungal burden (B) data from the Δ*tslA* strain are similar to the data from the wild-type and Δ*tslA*+*tslA* strains, while the loss of TslA increased inflammation (panels C and D and panels E and F). (A) A total of 10^6 conidia of each strain were inoculated via the intranasal route in a chemotherapeutic IPA murine model. Ten CD1 mice were used in each group. Survival analysis was performed for 2 weeks. p.i., postinfection. (B) No significant differences in fungal burden were observed in the strains tested. Analysis of the fungal burden of these mice was performed as previously described (36). (C) Δ*tslA*-infected lungs show more inflammatory cell infiltrations. The fungal histology was performed on day 2 and day 4 to observe the inflammatory cell infiltrations. Arrowheads show the abscess-like structure. Images are representative of results from three mice. Magnification, ×50. (D and E) Δ*tslA*-infected bronchoalveolar lavage fluid samples (BALs) had increased cell infiltrations, especially macrophages. To observe changes in the inflammatory response *in vivo*, cell counts and differential counts were performed. (D) *P* value = 0.0051 (unpaired two-tailed *t* test compared to the wild-type CEA10 results). (E) For neutrophils, *, $P < 0.05$ (two-tailed ANOVA for comparisons among the CEA10, Δ*tslA*, and Δ*tslA*+*tslA* strains); for macrophages, **, $P < 0.01$ (two-tailed ANOVA for comparisons among the CEA10, Δ*tslA*, and Δ*tslA*+*tslA* strains). (F) Luminex assay results from Δ*tslA* mutant-infected BALs show an increased inflammatory cytokine profile. Data are presented as means ± SE of results from BALF from three mice of each strain. *, *P* = 0.0286 (unpaired two-tailed Mann-Whitney test).

in a strain with an increase in virulence as measured by murine survival in a corticosteroid murine model of IPA (14). Though the mechanism for the increase in virulence is unknown, it is suggested to be driven by altered cell wall composition and immunopathogenesis (14). This result was rather surprising given that trehalose synthase null mutants in other human-pathogenic fungi are severely attenuated in virulence. In contrast, loss of the TPP Tps2 ortholog OrlA in *A. fumigatus* severely attenuated virulence in a chemotherapeutic murine model and markedly reduced virulence in an X-CGD murine model (15). As with the loss of TpsA and TpsB, the loss of OrlA

significantly alters the cell wall of *A. fumigatus*. Yet it has remained enigmatic how trehalose biosynthesis and cell wall biosynthesis are mechanistically linked.

To further explore the role of trehalose biosynthesis in *A. fumigatus* virulence and cell wall homeostasis, we identified and characterized two additional homologs of the *S. cerevisiae* trehalose biosynthesis complex, here named TslA and TslB. Our major finding is that *A. fumigatus* TslA physically interacts with the chitin synthase CsmA, which leads to a novel model where TslA can moonlight as a regulator of chitin biosynthesis. While our data do not rule out perturbations in carbon metabolism that occur upon loss of trehalose biosynthesis proteins impacting cell wall biosynthesis, they strongly suggest that TslA has a direct regulatory role through its interaction with the CsmA chitin synthase.

In *A. fumigatus*, TslA and TslB lack the canonical catalytic residues of both TPS and TPP domains, similarly to *S. cerevisiae* Tps3p (*Sc*Tps3p) and Tsl1p. Yet loss of TslA in *A. fumigatus* leads to a significant decrease in the trehalose content in both conidia and mycelia, similarly to the loss of *Sc*Tsl1p (11). Consequently, TslA is directly involved in regulating trehalose biosynthesis in *A. fumigatus*. Intriguingly, we observed a direct interaction between TslA and the *A. fumigatus* TPP (OrlA) in our experiments. Further experiments are needed to test the hypothesis that TslA serves as a regulator of TPP activity in *A. fumigatus*. In addition, trehalose assays of *tslA* and *tslB* null mutants suggest that while both TslA and TslB are involved in trehalose biosynthesis, these two proteins are not redundant and have multiple functions that remain to be fully elucidated in *A. fumigatus*.

The major phenotype associated with loss of TslA is a significant alteration in cell wall integrity as evidenced by cell wall stress assays. In addition, TEM and cell wall chitin and beta-glucan exposure assays strongly suggest that loss of TslA impacts cell wall homeostasis. To further understand the underlying mechanisms, we used an affinity purification approach followed by liquid chromatography-tandem mass spectrometry (LC-MS/MS) analysis of coprecipitating proteins with TslA. In *S. cerevisiae*, *Sc*Tsl1p and Tps3p interact with proteins that regulate cell wall rigidity and cell wall components in the spores, i.e., Pmt6p, an O-mannosyltransferase, and Sps2p (a protein expressed during sporulation), but there are no reports of interactions with cell wall biosynthesis enzymes (38). Surprisingly, however, we discovered that *A. fumigatus* TslA interacts with a class V chitin synthase, CsmA. To our knowledge, this is the first report of a protein-protein interaction between trehalose and cell wall biosynthesis proteins in fungi. However, *Sc*Tsl1p and Tps3p also interact with other enzymes in glycolysis, including other mitochondrial proteins. In our experiments, we also observed that TslA in *A. fumigatus* also interacts with enzymes in glycolysis, the pentose phosphate pathway, and mitochondrial proteins though these interactions remain to be validated.

Consequently, our data suggest that TslA plays a complex role in fungal carbon metabolism, cell wall homeostasis, and fungus-host interactions. For chitin production, G6P is converted into fructose 6-phosphate and then N-acetyl glucosamine, while UDP-glucose is the key building block to generate β-glucan. These substrates, G6P and UDP-glucose, are also the critical building blocks for trehalose biosynthesis. Perturbations in trehalose biosynthesis that occur when key proteins are lost through genetic mutation or in response to specific environments thus result in significant alterations in fungal carbon metabolism that may alter biosynthetic processes in the cell that require sugar-phosphate intermediates. Nevertheless, from the mRNA expression of the transcription factors in the cell wall integrity pathway (RlmA), the high-osmolarity glycerol–mitogen-activated protein kinase (HOG-MAPK) pathway (AtfA), the β-glucan synthase enzyme (FksA), and the class V chitin synthase enzyme (CsmA), we observed that the loss of TslA has no intrinsic effect on mRNA levels of these genes. These results suggest that the observed defects in cell wall homeostasis may be the result of the direct regulation of CsmA or other cell wall biosynthesis components by TslA.

A. fumigatus contains eight chitin synthase enzymes divided into seven classes (39, 40). However, only class V and class VII enzymes have an N-terminal myosin motor-like domain (MMD) (41–43). Fungal cells pack these enzymes into 60-nm-diameter mi-

crovesicles, called chitosomes, and transport them to the hyphal tip (44). Chitosomes merge with the apical cell membrane, and chitin synthase enzymes (Chs) are transported into the interior side of the cell membrane (45). However, MMD-Chs are also able to transport themselves along actin filaments to the fungal tip (34). In *Ustilago maydis*, chitosomes are not required for the cytoplasmic motility of class V chitin synthases (46, 47). MMD-Chs are usually found at the hyphal tip and septa, so they are proposed to be involved in polarized cell wall biosynthesis and septal formation (48). *A. fumigatus* possesses two chitin synthases with an MMD, called CsmA and CsmB (49). A *csmA* null mutant shows less chitin content in the conidial cell wall (49). Recently, Muszkieta et al. observed that CsmA is important for cell wall homeostasis (50). Loss of *csmA*, *csmB*, *chsF*, and *chsD* causes formation of a disorganized cell wall structure and significantly attenuates virulence *in vivo* (50).

In contrast, our results suggest that loss of TslA results in altered CsmA localization and an increase in chitin synthase activity. It is unknown how TslA binds to CsmA and affects its localization and activity. Localization of chitin synthase enzymes is essential for function, and their localization is dependent upon multiple regulatory steps, including posttranslational modifications, e.g., phosphorylation and dephosphorylation. For example, in *S. cerevisiae*, *Sc*Chs3 is phosphorylated by *Sc*Pkc1 under conditions of heat stress (51). *Sc*Sac1 phosphatase inhibits *Sc*Chs3 forward transportation, while *Sc*Pik1 overexpression promotes forward movement (52). Both *Sc*Sac1 and *Sc*Pik1 are important for Golgi trafficking to the plasma membrane (52). Furthermore, phosphorylation and dephosphorylation of *Sc*Chs3 are necessary for guiding Chs3 to the septum in each cell cycle stage (53). Lenardon et al. showed that *C. albicans* Chs3 (*Ca*Chs3), a major enzyme for chitin synthesis, is phosphorylated at Ser139 in *C. albicans* (54). Mutations at the site revealed that both phosphorylation and dephosphorylation of *Ca*Chs3 are crucial for the localization and function of *Ca*Chs3, including the polarized growth. However, kinases regulating phosphorylation of *Ca*Chs3 are still unknown (54). Consequently, it is possible that the mechanism behind altered CsmA localization in the absence of TslA is related to alteration of CsmA phosphorylation. In addition to the phosphorylation, as mentioned above, chitin synthase localization is also associated with actin filaments (34). Therefore, it is possible that TslA may stabilize the chitin synthase and actin complex to help direct localization and activity. We found from the LC-MS/MS data that TslA did not pull down ActA but did pull down an actin cytoskeleton protein (VIP1) and an actin-bundling protein (Sac6). Moreover, we observed that TslA localized in the cytosol along the hyphae without any obvious specific TslA localization sites, i.e., hyphal tips (Fig. 8D) (see Fig. S1 in the supplemental material). Furthermore, in filamentous fungi, microtubule-based intracellular trafficking plays an important role in the dynamics of various vesicles and proteins (55, 56). It is possible that CsmA localization is involved with both actin filaments and the microtubule-based mechanism (34). Additional research is needed to define the molecular mechanism through which TslA regulates CsmA localization and/or activity.

Importantly, the fungal cell wall is not only important for fungal survival but also essential for interactions with the host immune system (57). The balance between the host immune response and virulence of the fungi is an important factor that determines the fate of both fungal pathogens and hosts (57). Chitin plays an important role in the immune response to fungi. For example, chitin has an immunomodulatory effect on the host by shifting the immune response from a T_H1 response to a more T_H2-like response that can have an impact on fungal survival inside the host (58). Here, we observed increased levels of chitin exposure and content in the cell wall for *A. fumigatus* in the absence of TslA. We also noted the presence of electron-dense material on the exterior of Δ*tslA* hyphae. This electron-dense material could be galactosaminogalactan (GAG), a major component of the *A. fumigatus* extracellular matrix (59). GAG is an adhesin that is essential for biofilm formation (59, 60). GAG also has immunemodulatory effects inducing T_H2 lineage proliferation (59). Furthermore, exogenous GAG inhibits human proinflammatory cytokine production through interleukin-1 (IL-1) signaling by inducing IL-1 receptor antagonist (61). However, it remains unclear how

various cell wall compositions impact the inflammatory response and disease outcomes in IPA murine models. Therefore, additional studies are needed to investigate the connections among loss of TslA, cell wall components, and the observed altered host immune response. One translationally relevant future research direction is to examine the effects of TslA loss on the efficacy of a chitin synthase inhibitor such as nikkomycin Z. As TslA and other trehalose biosynthesis proteins have a profound effect on fungal cell wall homeostasis, further investigation into these molecular mechanisms may reveal novel targets or approaches for therapeutic development.

In conclusion, our results suggest that both TslA and TslB are involved in the biosynthesis of trehalose in *A. fumigatus*. However, the mechanisms behind the regulation of trehalose production by these two proteins are still unclear. What is clear is that TslA has an unexpected additional so-called moonlighting role in regulating chitin synthase activity. On the basis of the impact of TslA loss on CsmA localization, we speculate that TslA might be critical for the proper localization of key trehalose biosynthesis proteins such as OrlA. Importantly, these results strongly suggest that trehalose-related proteins are important for cell wall biosynthesis not only for their role in carbon metabolism regulation but also from direct physical interactions with cell wall biosynthesis enzymes. A more fundamental understanding of the underlying mechanisms linking trehalose and cell wall biosynthesis may uncover potential novel antifungal targets and will enhance our understanding of *A. fumigatus*-host interactions.

MATERIALS AND METHODS

Fungal strains, media, and growth conditions. *Aspergillus fumigatus* strain CEA17 (a uracil auxotroph strain lacking a *pyrG* gene) was used to generate *tslA*, *tslB*, and *tslA/B* null mutants (62). A *ku80* strain (a uracil auxotroph strain lacking *pyrG* and *akuB* genes) was used to generate S-tagged and Flag-tagged strains for pulldown and coimmunoprecipitation experiments (62, 63). Glucose minimal media (GMM) containing 1% glucose were used to grow the mutants along with a wild-type strain, CEA10 (CBS144.89), at 37°C in 5% CO_2 if not stated otherwise (64). The conidia from each strain were collected by the use of 0.01% Tween 80 after 72 h of incubation at 37°C in 5% CO_2. Fresh conidia were used in all experiments.

Strain construction and fungal transformation. Gene replacements and reconstituted strains were generated as previously described (15, 35). All strains are listed in Table S1 in the supplemental material. PCR and Southern blotting were used to confirm the mutant strains (15). Real-time reverse transcriptase PCR was used to confirm expression of the reintroduced gene (65). To generate the single-null mutant, *A. parasiticus pyrG* from pJW24 was used as a selectable marker (20). To generate a double-null mutant strain and reconstituted strains of single-null mutants, we utilized a *ptrA* marker, which is a pyrithiamine resistance gene from *A. oryzae* (21). To generate reconstituted strains of the double-null mutant, we utilized *hygB*, which is a hygromycin B phosphotransferase gene, as a hygromycin resistance marker (22). For S-tagged strains, an S-tag coding sequence was introduced along with *A. fumigatus pyrG* (*AfpyrG*) into the C terminus of proteins of interest, i.e., TslA and TslB (30, 31). For coimmunoprecipitation experiments, we introduced a Flag tag together with *ptrA* as a marker into the C terminus at the loci encoding proteins of interest, e.g., CsmA, in the TslA-S tag background (66). In localization experiments, we generated C-terminal GFP-tagged CsmA in both the wild-type (CEA17) and Δ*tslA* strain backgrounds by using *pyrG* and *ptrA* as selectable markers, respectively. After the constructs were generated, polyethylene glycol-mediated transformation of fungal protoplasts was performed as previously described (67). For the *ptrA marker* transformation, we added pyrithiamine hydrobromide (Sigma; catalog no. P0256) to 1.2 M sorbitol media (sorbitol minimal media [SMM]) at 0.1 mg/liter (21). For the *hygB marker* transformation, we recovered the strains containing the *hygB* marker by adding hygromycin B (Calbiochem; catalog no. 400052) into the 0.7% SMM agar overlay at 150 μg/ml the day after transformation (22).

Trehalose measurement. Trehalose content in conidia and mycelia was measured as previously described (15). Briefly, a total of 2×10^8 conidia were used for the conidial stage of the trehalose assay, and 1×10^8 conidia were cultured overnight in 10 ml liquid glucose minimal medium (LGMM) for the mycelial stage as described by d'Enfert and Fontaine (1997) (68). Cell-free extracts were then tested for trehalose levels according to the glucose assay kit protocols (Sigma; catalog no. GAGO20). Results from biological triplicate experiments were averaged, standard deviation calculated, and statistical significance determined ($P < 0.05$) with an unpaired two-tailed Student's *t* test.

Cell wall-perturbing agents and antifungal agents. Several cell wall-perturbing agents, namely, Congo red (CR) (Sigma catalog no. C6277), calcofluor white (CFW) (fluorescent brightener 28; Sigma catalog no. F3543), and caspofungin (CPG) (Cancidas; Merck & Co., Inc.), were utilized for cell wall integrity tests. CR, CFW, or CPG was added into GMM plates at a final concentration of 1 mg/ml, 50 μg/ml, or 1 μg/ml, respectively. Dropout assays were performed by plating serial dilutions of 1×10^5 to 1×10^2 conidia in a 5-μl drop of each strain. The plates were cultured at 37°C in 5% CO_2, and the images were taken at 48 h. This experiment was performed in three biological replicates (15).

Cell wall MAMP exposure. Calcofluor white (CFW), fluorescein-labeled wheat germ agglutinin (WGA) (Vector Laboratories; catalog no. FL-1021), and soluble dectin-1 staining was performed as

previously described (58, 69). Briefly, each fungal strain was cultured until it reached the germination stage on liquid glucose minimal media. The hyphae were UV irradiated at 6,000 mJ/cm^2. The micrographs were taken using the Z-stack of the fluorescence microscope, a Zeiss HAL 100 microscope (Carl Zeiss Microscopy LLC, Thornwood, NY), equipped with a Zeiss AxioCam MRm camera. The intensity was analyzed using ImageJ, and the corrected total cell fluorescence (CTCF) was calculated (69, 70). Data are presented as means ± standard errors (SE) corresponding to 15 images from three biological replicates.

Transmission electron microscopy. The cell walls of the wild-type strain (CEA10) and the Δ*tslA* and Δ*tslA*+*tslA* strains were examined by using TEM as previously described (19, 39). All TEM images were taken at 100 kV on a JEOL TEM 1010 microscope (JEOL, Tokyo, Japan) equipped with a digital camera (XR-41B; Advanced Microscopy Techniques). Cell wall thickness was analyzed using ImageJ (69). Data are presented as means ± SE of 10 measurements from two biological replicates of each strain.

Proteomic assay, pulldown assay, and coimmunoprecipitation. In the pulldown assays for the S tag, 10^8 conidia of the wild-type and S-tagged strains were incubated in 100 ml liquid GMM medium at 30°C for 8 h and switched to 37°C for 16 h (250 rpm). The mycelia from each strain were collected and lyophilized overnight. Proteins were extracted as previously described (30). Sample supernatants were measured to estimate protein concentrations using the Bradford method (Bio-Rad, Hercules, CA). For the purification step, 300 μl of S protein agarose slurry (Novagen) (150-μl packed bead volume) was added per 100 mg of protein and incubated at 4°C using rotary agitation for 1 h and previously described purification steps (30). The supernatant was loaded into 10% mini-protein precast gels (Bio-Rad). The gel was stained with Bio-Safe Coomassie blue (Bio-Rad) for 3 h. The bands were cut and submitted for mass spectrometry analysis (LC-MS/MS) at The Vermont Genetics Network, University of Vermont, Burlington, VT.

Co-IP with *S*-protein beads and anti-Flag magnetic beads. To perform coimmunoprecipitation assays, C-terminal Flag-tagged CsmA strains were generated in the S-tagged TslA background. S-protein bead Co-IP experiments were performed in the same way as the previously described S-protein bead pulldown experiments. To perform reciprocal coimmunoprecipitation assays, C-terminal Flag-tagged CsmA strains were used. An IP buffer was used followed by affinity purifications with anti-Flag M2 magnetic beads (Sigma) as previously described (66). Proteins were transferred from a 10% SDS-PAGE gel onto a polyvinylidene difluoride (PVDF) membrane for a Western blot assay using a Trans-Blot turbo transfer system (Bio-Rad). S-tagged TslA was detected using a rabbit anti-S-tag antibody (ICL) at 1:5,000 dilution and a goat anti-rabbit IgG (H+L) horseradish peroxidase (HRP) antibody (Thermo Scientific) at 1:10,000 dilution. For the Flag-tagged CsmA, a mouse monoclonal anti-Flag M2 antibody (F1804; Sigma) was used at 1:10,000 dilution as a primary antibody followed by an anti-mouse IgG HRP conjugate (W4021; Promega) used at 1:2,500 dilution as a secondary antibody. Chemiluminescence detection was performed using a Clarity Western ECL substrate (Bio-Rad) and a FluorChem FC2 imager (Alpha Innotech). For loading controls, an anti-tubulin antibody (Sigma; catalog no. T5192) (human) was utilized.

Chitin synthase activity assay. A total of 10^8 conidia of each fungal strain were grown at 37°C for 24 h in 10 ml of liquid GMM at 250 rpm. The mycelia were collected for preparation of membrane fractions by centrifugation at 100,000 × *g* for 40 min at 4°C as described before. After that, the nonradioactive chitin synthase activity assay was performed in a 96-well plate as previously described (32, 33).

Murine model of invasive pulmonary aspergillosis. CD1 female mice (6 to 8 weeks old) were used in chemotherapeutic murine model experiments as previously described (35). Mice were obtained from Charles River Laboratories, Inc. (Raleigh, NC). For survival studies and histopathology, 10 mice per *A. fumigatus* strain (including strains CEA10, Δ*tslA*, and Δ*tslA*+*tslA*) were inoculated intranasally with 1×10^6 conidia in 40 μl of phosphate-buffered saline (PBS) and monitored three times a day. Mice were observed for 14 days after the *A. fumigatus* challenge. Any animals showing distress were immediately humanely sacrificed and recorded as deaths within 24 h. No mock-infected animals perished in any of the experiments. Statistical comparison of the associated Kaplan-Meier curves was conducted with log rank tests (71). Lungs were removed from all mice sacrificed at different time points during the experiment for fungal burden assessment and histopathology.

Histopathology. The chemotherapeutic murine model was performed additionally for histopathology. Three mice in each group (including the CEA10, Δ*tslA*, and Δ*tslA*+*tslA* strain groups) were humanely euthanized at day 2 and day 4 postinoculation. Lungs were harvested from each group and fixed in 10% formalin before embedding in paraffin was performed. Sections (5 μm in thickness) were taken and stained with either H&E (hematoxylin and eosin) or GMS (Gomori's methenamine silver stain) as previously described (72). Slides were analyzed microscopically with a Zeiss Axioplan 2 imaging microscope (Carl Zeiss Microimaging, Inc., Thornwood, NY) fitted with a QImaging Retiga-SRV Fast 1394 red-green-blue (RGB) camera. The analysis was performed in Phylum Live 4 imaging software. Images were captured at ×50 magnification as indicated in each image.

***In vivo* fungal burden.** Quantitative analysis of fungal growth in infected mouse lungs was performed after lungs were harvested at day 4 postinoculation with a quantitative PCR as previously described (36). Values were averaged for the CEA10, Δ*tslA*, and Δ*tslA*+*tslA* strains at each time point and compared using the Mann-Whitney-corrected *t* test.

Collection and analysis of bronchoalveolar lavage fluid (BALF). At the indicated time after *A. fumigatus* instillation, mice were euthanized using CO_2. Bronchoalveolar lavage fluid (BALF) was collected by washing the lungs with 2 ml of PBS containing 0.05 M EDTA. BALF was then centrifuged and the supernatant collected and stored at −20°C until analysis. BAL fluid cells were resuspended in 200 μl of PBS and counted on a hemocytometer to determine total cell counts. Cells were then spun onto glass slides using a Thermo Scientific Cytospin4 cytocentrifuge and were subsequently stained using a

Diff-Quik staining kit (Electron Microscopy Sciences) for differential cell counting. Assays for analysis of cytokines and chemokines from BALF were performed by using a Luminex system as previously described (69).

Ethics statement. This study was carried out in strict accordance with the recommendations given in the *Guide for the Care and Use of Laboratory Animals* of the National Institutes of Health. The animal experimental protocol was approved by the Institutional Animal Care and Use Committee (IACUC) at Dartmouth College (protocol number cram.ra.1).

Statistical analysis. All statistical analyses were done with Prism 5 software (GraphPad Software, Inc., San Diego, CA). All error bars represent standard errors of the means.

SUPPLEMENTAL MATERIAL

Supplemental material for this article may be found at https://doi.org/10.1128/mBio.00056-17.

FIG S1, TIF file, 2.4 MB.

TABLE S1, DOCX file, 0.1 MB.

TABLE S2, XLSX file, 0.4 MB.

ACKNOWLEDGMENTS

We thank the members of the Vermont Genomics Network, UVM, for LC-MS/MS analysis (INBRE8P20GM103449) and the members of the microscope facilities of the Department of Biology at Dartmouth College and of the electron microscopy facilities at Dartmouth College for analyzing TEM images. A.T. thanks Dawoon Chung for initial training in *A. fumigatus* molecular genetics techniques. A.T. and R.A.C. thank Jarrod Fortwendel for the chitin synthase activity assay protocol and Thomas Hampton for suggestions on statistical analysis.

This work, including the efforts of R.A.C., was funded by HHS, NIH, National Institute of Allergy and Infectious Diseases (NIAID) (R01 AI081838). R.A.C. holds an Investigators in the Pathogenesis of Infectious Diseases Award from the Burroughs Wellcome Fund (BWF). Additional support came from a National Institute of General Medicine Sciences (NIGMS) award (P30GM106394) (Bruce Stanton, principal investigator) and a Cystic Fibrosis Foundation award (Bruce Stanton, principal investigator). A.T. is supported by a fellowship from the Department of Microbiology, Faculty of Medicine, Chulalongkorn University, Bangkok, Thailand.

REFERENCES

1. Dagenais TR, Keller NP. 2009. Pathogenesis of *Aspergillus fumigatus* in invasive aspergillosis. Clin Microbiol Rev 22:447–465. https://doi.org/10.1128/CMR.00055-08.
2. Patterson TF, Thompson GR, III, Denning DW, Fishman JA, Hadley S, Herbrecht R, Kontoyiannis DP, Marr KA, Morrison VA, Nguyen MH, Segal BH, Steinbach WJ, Stevens DA, Walsh TJ, Wingard JR, Young JA, Bennett JE. 2016. Practice guidelines for the diagnosis and management of aspergillosis: 2016 update by the Infectious Diseases Society of America. Clin Infect Dis 63:e1–e60. https://doi.org/10.1093/cid/ciw326.
3. Verweij PE, Snelders E, Kema GH, Mellado E, Melchers WJ. 2009. Azole resistance in *Aspergillus fumigatus*: a side-effect of environmental fungicide use? Lancet Infect Dis 9:789–795. https://doi.org/10.1016/S1473-3099(09)70265-8.
4. Verweij PE, Chowdhary A, Melchers WJ, Meis JF. 2016. Azole resistance in *Aspergillus fumigatus*: can we retain the clinical use of mold-active antifungal azoles? Clin Infect Dis 62:362–368. https://doi.org/10.1093/cid/civ885.
5. Leloir LF, Cabib E. 1953. The enzymic synthesis of trehalose phosphate. J Am Chem Soc 75:5445–5446. https://doi.org/10.1021/ja01117a528.
6. Cabib E, Leloir LF. 1958. The biosynthesis of trehalose phosphate. J Biol Chem 231:259–275.
7. Vuorio OE, Kalkkinen N, Londesborough J. 1993. Cloning of two related genes encoding the 56-kDa and 123-kDa subunits of trehalose synthase from the yeast *Saccharomyces cerevisiae*. Eur J Biochem 216:849–861. https://doi.org/10.1111/j.1432-1033.1993.tb18207.x.
8. Elliott B, Haltiwanger RS, Futcher B. 1996. Synergy between trehalose and Hsp104 for thermotolerance in *Saccharomyces cerevisiae*. Genetics 144:923–933.
9. Gancedo C, Flores CL. 2004. The importance of a functional trehalose biosynthetic pathway for the life of yeasts and fungi. FEMS Yeast Res 4:351–359. https://doi.org/10.1016/S1567-1356(03)00222-8.
10. Londesborough J, Vuorio OE. 1993. Purification of trehalose synthase from baker's yeast. Its temperature-dependent activation by fructose 6-phosphate and inhibition by phosphate. Eur J Biochem 216:841–848. https://doi.org/10.1111/j.1432-1033.1993.tb18206.x.
11. Ferreira JC, Silva JT, Panek AD. 1996. A regulatory role for *TSL1* on trehalose synthase activity. Biochem Mol Biol Int 38:259–265.
12. Zaragoza O, Blazquez MA, Gancedo C. 1998. Disruption of the *Candida albicans TPS1* gene encoding trehalose-6-phosphate synthase impairs formation of hyphae and decreases infectivity. J Bacteriol 180:3809–3815.
13. Petzold EW, Himmelreich U, Mylonakis E, Rude T, Toffaletti D, Cox GM, Miller JL, Perfect JR. 2006. Characterization and regulation of the trehalose synthesis pathway and its importance in the pathogenicity of *Cryptococcus neoformans*. Infect Immun 74:5877–5887. https://doi.org/10.1128/IAI.00624-06.
14. Al-Bader N, Vanier G, Liu H, Gravelat FN, Urb M, Hoareau CM, Campoli P, Chabot J, Filler SG, Sheppard DC. 2010. Role of trehalose biosynthesis in *Aspergillus fumigatus* development, stress response, and virulence. Infect Immun 78:3007–3018. https://doi.org/10.1128/IAI.00813-09.
15. Puttikamonkul S, Willger SD, Grahl N, Perfect JR, Movahed N, Bothner B, Park S, Paderu P, Perlin DS, Cramer RA, Jr. 2010. Trehalose 6-phosphate phosphatase is required for cell wall integrity and fungal virulence but not trehalose biosynthesis in the human fungal pathogen *Aspergillus fumigatus*. Mol Microbiol 77:891–911. https://doi.org/10.1111/j.1365-2958.2010.07254.x.
16. Svanström Å, van Leeuwen MR, Dijksterhuis J, Melin P. 2014. Trehalose synthesis in *Aspergillus niger*: characterization of six homologous genes,

all with conserved orthologs in related species. BMC Microbiol 14:90. https://doi.org/10.1186/1471-2180-14-90.
17. Gibson RP, Turkenburg JP, Charnock SJ, Lloyd R, Davies GJ. 2002. Insights into trehalose synthesis provided by the structure of the retaining glucosyltransferase OtsA. Chem Biol 9:1337–1346. https://doi.org/10.1016/S1074-5521(02)00292-2.
18. Rao KN, Kumaran D, Seetharaman J, Bonanno JB, Burley SK, Swaminathan S. 2006. Crystal structure of trehalose-6-phosphate phosphatase-related protein: biochemical and biological implications. Protein Sci 15:1735–1744. https://doi.org/10.1110/ps.062096606.
19. Willger SD, Puttikamonkul S, Kim KH, Burritt JB, Grahl N, Metzler LJ, Barbuch R, Bard M, Lawrence CB, Cramer RA, Jr. 2008. A sterol-regulatory element binding protein is required for cell polarity, hypoxia adaptation, azole drug resistance, and virulence in *Aspergillus fumigatus*. PLoS Pathog 4:e1000200. https://doi.org/10.1371/journal.ppat.1000200.
20. Weidner G, d'Enfert C, Koch A, Mol PC, Brakhage AA. 1998. Development of a homologous transformation system for the human pathogenic fungus *Aspergillus fumigatus* based on the pyrG gene encoding orotidine 5′-monophosphate decarboxylase. Curr Genet 33:378–385. https://doi.org/10.1007/s002940050350.
21. Kubodera T, Yamashita N, Nishimura A. 2002. Transformation of *Aspergillus* sp. and *Trichoderma reesei* using the pyrithiamine resistance gene (*ptrA*) of *Aspergillus oryzae*. Biosci Biotechnol Biochem 66:404–406. https://doi.org/10.1271/bbb.66.404.
22. Cullen D, Leong SA, Wilson LJ, Henner DJ. 1987. Transformation of *Aspergillus nidulans* with the hygromycin-resistance gene, *hph*. Gene 57:21–26. https://doi.org/10.1016/0378-1119(87)90172-7.
23. Fillinger S, Chaveroche MK, van Dijck P, de Vries R, Ruijter G, Thevelein J, d'Enfert C. 2001. Trehalose is required for the acquisition of tolerance to a variety of stresses in the filamentous fungus *Aspergillus nidulans*. Microbiology 147:1851–1862. https://doi.org/10.1099/00221287-147-7-1851.
24. Rocha MC, Fabri JH, Franco de Godoy K, Alves de Castro P, Hori JI, Ferreira da Cunha A, Arentshorst M, Ram AF, van den Hondel CA, Goldman GH, Malavazi I. 2016. *Aspergillus fumigatus* MADS-Box transcription factor *rlmA* is required for regulation of the cell wall integrity and virulence. G3 6:2983–3002. https://doi.org/10.1534/g3.116.031112.
25. Hagiwara D, Suzuki S, Kamei K, Gonoi T, Kawamoto S. 2014. The role of AtfA and HOG MAPK pathway in stress tolerance in conidia of *Aspergillus fumigatus*. Fungal Genet Biol 73:138–149. https://doi.org/10.1016/j.fgb.2014.10.011.
26. Mazur P, Morin N, Baginsky W, el-Sherbeini M, Clemas JA, Nielsen JB, Foor F. 1995. Differential expression and function of two homologous subunits of yeast 1,3-beta-D-glucan synthase. Mol Cell Biol 15:5671–5681. https://doi.org/10.1128/MCB.15.10.5671.
27. Yoshimi A, Sano M, Inaba A, Kokubun Y, Fujioka T, Mizutani O, Hagiwara D, Fujikawa T, Nishimura M, Yano S, Kasahara S, Shimizu K, Yamaguchi M, Kawakami K, Abe K. 2013. Functional analysis of the alpha-1,3-glucan synthase genes agsA and agsB in *Aspergillus nidulans*: agsB is the major alpha-1,3-glucan synthase in this fungus. PLoS One 8:e54893. https://doi.org/10.1371/journal.pone.0054893.
28. Beauvais A, Fontaine T, Aimanianda V, Latgé JP. 2014. *Aspergillus* cell wall and biofilm. Mycopathologia 178:371–377. https://doi.org/10.1007/s11046-014-9766-0.
29. Barker BM, Kroll K, Vödisch M, Mazurie A, Kniemeyer O, Cramer RA. 2012. Transcriptomic and proteomic analyses of the *Aspergillus fumigatus* hypoxia response using an oxygen-controlled fermenter. BMC Genomics 13:62. https://doi.org/10.1186/1471-2164-13-62.
30. Liu HL, Osmani AH, Ukil L, Son S, Markossian S, Shen KF, Govindaraghavan M, Varadaraj A, Hashmi SB, De Souza CP, Osmani SA. 2010. Single-step affinity purification for fungal proteomics. Eukaryot Cell 9:831–833. https://doi.org/10.1128/EC.00032-10.
31. Liu HL, De Souza CP, Osmani AH, Osmani SA. 2009. The three fungal transmembrane nuclear pore complex proteins of *Aspergillus nidulans* are dispensable in the presence of an intact An-Nup84-120 complex. Mol Biol Cell 20:616–630. https://doi.org/10.1091/mbc.E08-06-0628.
32. Fortwendel JR, Juvvadi PR, Perfect BZ, Rogg LE, Perfect JR, Steinbach WJ. 2010. Transcriptional regulation of chitin synthases by calcineurin controls paradoxical growth of *Aspergillus fumigatus* in response to caspofungin. Antimicrob Agents Chemother 54:1555–1563. https://doi.org/10.1128/AAC.00854-09.
33. Lucero HA, Kuranda MJ, Bulik DA. 2002. A nonradioactive, high throughput assay for chitin synthase activity. Anal Biochem 305:97–105. https://doi.org/10.1006/abio.2002.5594.
34. Takeshita N, Ohta A, Horiuchi H. 2005. CsmA, a class V chitin synthase with a myosin motor-like domain, is localized through direct interaction with the actin cytoskeleton in *Aspergillus nidulans*. Mol Biol Cell 16:1961–1970. https://doi.org/10.1091/mbc.E04-09-0761.
35. Grahl N, Puttikamonkul S, Macdonald JM, Gamcsik MP, Ngo LY, Hohl TM, Cramer RA. 2011. In vivo hypoxia and a fungal alcohol dehydrogenase influence the pathogenesis of invasive pulmonary aspergillosis. PLoS Pathog 7:e1002145. https://doi.org/10.1371/journal.ppat.1002145.
36. Li H, Barker BM, Grahl N, Puttikamonkul S, Bell JD, Craven KD, Cramer RA, Jr. 2011. The small GTPase RacA mediates intracellular reactive oxygen species production, polarized growth, and virulence in the human fungal pathogen *Aspergillus fumigatus*. Eukaryot Cell 10:174–186. https://doi.org/10.1128/EC.00288-10.
37. Foster AJ, Jenkinson JM, Talbot NJ. 2003. Trehalose synthesis and metabolism are required at different stages of plant infection by *Magnaporthe grisea*. EMBO J 22:225–235. https://doi.org/10.1093/emboj/cdg018.
38. Costanzo M, Baryshnikova A, Bellay J, Kim Y, Spear ED, Sevier CS, Ding H, Koh JL, Toufighi K, Mostafavi S, Prinz J, St Onge RP, VanderSluis B, Makhnevych T, Vizeacoumar FJ, Alizadeh S, Bahr S, Brost RL, Chen Y, Cokol M, Deshpande R, Li Z, Lin ZY, Liang W, Marback M, Paw J, San Luis BJ, Shuteriqi E, Tong AH, van Dyk N, Wallace IM, Whitney JA, Weirauch MT, Zhong G, Zhu H, Houry WA, Brudno M, Ragibizadeh S, Papp B, Pál C, Roth FP, Giaever G, Nislow C, Troyanskaya OG, Bussey H, Bader GD, Gingras AC, Morris QD, Kim PM, Kaiser CA. 2010. The genetic landscape of a cell. Science 327:425–431. https://doi.org/10.1126/science.1180823.
39. Bernard M, Latgé JP. 2001. *Aspergillus fumigatus* cell wall: composition and biosynthesis. Med Mycol 39(Suppl 1):9–17. https://doi.org/10.1080/mmy.39.1.9.17.
40. Munro CA, Gow NA. 2001. Chitin synthesis in human pathogenic fungi. Med Mycol 39(Suppl 1):41–53. https://doi.org/10.1080/mmy.39.1.41.53.
41. Choquer M, Boccara M, Gonçalves IR, Soulié MC, Vidal-Cros A. 2004. Survey of the *Botrytis cinerea* chitin synthase multigenic family through the analysis of six euascomycetes genomes. Eur J Biochem 271:2153–2164. https://doi.org/10.1111/j.1432-1033.2004.04135.x.
42. Din AB, Specht CA, Robbins PW, Yarden O. 1996. chs-4, a class IV chitin synthase gene from *Neurospora crassa*. Mol Gen Genet 250:214–222.
43. Fujiwara M, Horiuchi H, Ohta A, Takagi M. 1997. A novel fungal gene encoding chitin synthase with a myosin motor-like domain. Biochem Biophys Res Commun 236:75–78. https://doi.org/10.1006/bbrc.1997.6907.
44. Leal-Morales CA, Bracker CE, Bartnicki-Garcia S. 1988. Localization of chitin synthetase in cell-free homogenates of *Saccharomyces cerevisiae*: chitosomes and plasma membrane. Proc Natl Acad Sci U S A 85:8516–8520. https://doi.org/10.1073/pnas.85.22.8516.
45. Riquelme M. 2013. Tip growth in filamentous fungi: a road trip to the apex. Annu Rev Microbiol 67:587–609. https://doi.org/10.1146/annurev-micro-092412-155652.
46. Treitschke S, Doehlemann G, Schuster M, Steinberg G. 2010. The myosin motor domain of fungal chitin synthase V is dispensable for vesicle motility but required for virulence of the maize pathogen *Ustilago maydis*. Plant Cell 22:2476–2494. https://doi.org/10.1105/tpc.110.075028.
47. Steinberg G. 2011. Motors in fungal morphogenesis: cooperation versus competition. Curr Opin Microbiol 14:660–667. https://doi.org/10.1016/j.mib.2011.09.013.
48. Fajardo-Somera RA, Jöhnk B, Bayram Ö, Valerius O, Braus GH, Riquelme M. 2015. Dissecting the function of the different chitin synthases in vegetative growth and sexual development in *Neurospora crassa*. Fungal Genet Biol 75:30–45. https://doi.org/10.1016/j.fgb.2015.01.002.
49. Jiménez-Ortigosa C, Aimanianda V, Muszkieta L, Mouyna I, Alsteens D, Pire S, Beau R, Krappmann S, Beauvais A, Dufrêne YF, Roncero C, Latgé JP. 2012. Chitin synthases with a myosin motor-like domain control the resistance of *Aspergillus fumigatus* to echinocandins. Antimicrob Agents Chemother 56:6121–6131. https://doi.org/10.1128/AAC.00752-12.
50. Muszkieta L, Aimanianda V, Mellado E, Gribaldo S, Alcàzar-Fuoli L, Szewczyk E, Prevost MC, Latgé JP. 2014. Deciphering the role of the chitin synthase families 1 and 2 in the in vivo and in vitro growth of *Aspergillus fumigatus* by multiple gene targeting deletion. Cell Microbiol 16:1784–1805. https://doi.org/10.1111/cmi.12326.
51. Valdivia RH, Schekman R. 2003. The yeasts Rho1p and Pkc1p regulate the transport of chitin synthase III (Chs3p) from internal stores to the plasma membrane. Proc Natl Acad Sci U S A 100:10287–10292. https://doi.org/10.1073/pnas.1834246100.
52. Schorr M, Then A, Tahirovic S, Hug N, Mayinger P. 2001. The phosphoinositide phosphatase Sac1p controls trafficking of the yeast Chs3p

chitin synthase. Curr Biol 11:1421–1426. https://doi.org/10.1016/S0960-9822(01)00449-3.
53. Reyes A, Sanz M, Duran A, Roncero C. 2007. Chitin synthase III requires Chs4p-dependent translocation of Chs3p into the plasma membrane. J Cell Sci 120:1998–2009. https://doi.org/10.1242/jcs.005124.
54. Lenardon MD, Milne SA, Mora-Montes HM, Kaffarnik FA, Peck SC, Brown AJ, Munro CA, Gow NA. 2010. Phosphorylation regulates polarisation of chitin synthesis in *Candida albicans*. J Cell Sci 123:2199–2206. https://doi.org/10.1242/jcs.060210.
55. Xiang X, Plamann M. 2003. Cytoskeleton and motor proteins in filamentous fungi. Curr Opin Microbiol 6:628–633. https://doi.org/10.1016/j.mib.2003.10.009.
56. Zhang J, Li S, Fischer R, Xiang X. 2003. Accumulation of cytoplasmic dynein and dynactin at microtubule plus ends in *Aspergillus nidulans* is kinesin dependent. Mol Biol Cell 14:1479–1488. https://doi.org/10.1091/mbc.E02-08-0516.
57. Shepardson KM, Cramer RA. 2013. Fungal cell wall dynamics and infection site microenvironments: signal integration and infection outcome. Curr Opin Microbiol 16:385–390. https://doi.org/10.1016/j.mib.2013.03.003.
58. Wagener J, Malireddi RK, Lenardon MD, Köberle M, Vautier S, MacCallum DM, Biedermann T, Schaller M, Netea MG, Kanneganti TD, Brown GD, Brown AJ, Gow NA. 2014. Fungal chitin dampens inflammation through IL-10 induction mediated by NOD2 and TLR9 activation. PLoS Pathog 10:e1004050. https://doi.org/10.1371/journal.ppat.1004050.
59. Fontaine T, Delangle A, Simenel C, Coddeville B, van Vliet SJ, van Kooyk Y, Bozza S, Moretti S, Schwarz F, Trichot C, Aebi M, Delepierre M, Elbim C, Romani L, Latgé JP. 2011. Galactosaminogalactan, a new immunosuppressive polysaccharide of *Aspergillus fumigatus*. PLoS Pathog 7:e1002372. https://doi.org/10.1371/journal.ppat.1002372.
60. Gravelat FN, Beauvais A, Liu H, Lee MJ, Snarr BD, Chen D, Xu W, Kravtsov I, Hoareau CM, Vanier G, Urb M, Campoli P, Al Abdallah Q, Lehoux M, Chabot JC, Ouimet MC, Baptista SD, Fritz JH, Nierman WC, Latgé JP, Mitchell AP, Filler SG, Fontaine T, Sheppard DC. 2013. *Aspergillus* galactosaminogalactan mediates adherence to host constituents and conceals hyphal beta-glucan from the immune system. PLoS Pathog 9:e1003575. https://doi.org/10.1371/journal.ppat.1003575.
61. Gresnigt MS, Bozza S, Becker KL, Joosten LA, Abdollahi-Roodsaz S, van der Berg WB, Dinarello CA, Netea MG, Fontaine T, De Luca A, Moretti S, Romani L, Latge JP, van de Veerdonk FL. 2014. A polysaccharide virulence factor from *Aspergillus fumigatus* elicits anti-inflammatory effects through induction of interleukin-1 receptor antagonist. PLoS Pathog 10:e1003936. https://doi.org/10.1371/journal.ppat.1003936.
62. d'Enfert C. 1996. Selection of multiple disruption events in *Aspergillus fumigatus* using the orotidine-5′-decarboxylase gene, *pyrG*, as a unique transformation marker. Curr Genet 30:76–82. https://doi.org/10.1007/s002940050103.
63. da Silva Ferreira ME, Kress MR, Savoldi M, Goldman MH, Härtl A, Heinekamp T, Brakhage AA, Goldman GH. 2006. The *akuB* (*KU80*) mutant deficient for nonhomologous end joining is a powerful tool for analyzing pathogenicity in *Aspergillus fumigatus*. Eukaryot Cell 5:207–211. https://doi.org/10.1128/EC.5.1.207-211.2006.
64. Shimizu K, Keller NP. 2001. Genetic involvement of a cAMP-dependent protein kinase in a G protein signaling pathway regulating morphological and chemical transitions in *Aspergillus nidulans*. Genetics 157:591–600.
65. Cramer RA, Jr, Gamcsik MP, Brooking RM, Najvar LK, Kirkpatrick WR, Patterson TF, Balibar CJ, Graybill JR, Perfect JR, Abraham SN, Steinbach WJ. 2006. Disruption of a nonribosomal peptide synthetase in *Aspergillus fumigatus* eliminates gliotoxin production. Eukaryot Cell 5:972–980. https://doi.org/10.1128/EC.00049-06.
66. Franceschetti M, Bueno E, Wilson RA, Tucker SL, Gómez-Mena C, Calder G, Sesma A. 2011. Fungal virulence and development is regulated by alternative pre-mRNA 3′end processing in *Magnaporthe oryzae*. PLoS Pathog 7:e1002441. https://doi.org/10.1371/journal.ppat.1002441.
67. Bok JW, Keller NP. 2004. LaeA, a regulator of secondary metabolism in *Aspergillus* spp. Eukaryot Cell 3:527–535. https://doi.org/10.1128/EC.3.2.527-535.2004.
68. d'Enfert C, Fontaine T. 1997. Molecular characterization of the *Aspergillus nidulans treA* gene encoding an acid trehalase required for growth on trehalose. Mol Microbiol 24:203–216. https://doi.org/10.1046/j.1365-2958.1997.3131693.x.
69. Shepardson KM, Ngo LY, Aimanianda V, Latgé JP, Barker BM, Blosser SJ, Iwakura Y, Hohl TM, Cramer RA. 2013. Hypoxia enhances innate immune activation to *Aspergillus fumigatus* through cell wall modulation. Microbes Infect 15:259–269. https://doi.org/10.1016/j.micinf.2012.11.010.
70. Gavet O, Pines J. 2010. Progressive activation of CyclinB1-Cdk1 coordinates entry to mitosis. Dev Cell 18:533–543. https://doi.org/10.1016/j.devcel.2010.02.013.
71. Willger SD, Cornish EJ, Chung D, Fleming BA, Lehmann MM, Puttikamonkul S, Cramer RA. 2012. Dsc orthologs are required for hypoxia adaptation, triazole drug responses, and fungal virulence in *Aspergillus fumigatus*. Eukaryot Cell 11:1557–1567. https://doi.org/10.1128/EC.00252-12.
72. Huppert M, Oliver DJ, Sun SH. 1978. Combined methenamine-silver nitrate and hematoxylin & eosin stain for fungi in tissues. J Clin Microbiol 8:598–603.